

CLOSED-FORM DESIGN FORMULATIONS OF ARBITRARY PHASE DELAY CROSSOVER BASED ON ADMITTANCE MATRIX

Ge Tian^{1, *}, Jin-Ping Yang², and Wen Wu¹

¹Ministerial Key Laboratory of JGMT, Nanjing University of Science and Technology, Nanjing 210094, China

²Purple Mountain Observatory, CAS, Nanjing 210008, China

Abstract—A design method for four-port crossover with arbitrary phase delay is proposed in this paper. This method is based on admittance matrix. Closed-form design formulations are deduced by making the structure admittance matrix equal to theoretical one. A crossover with 45° phase delay is designed and fabricated for theory verification. In the Butler beam forming network, this crossover has two functions for making the elimination of the 45° phase shifter possible and being used for circuit layout. Thus compact structure and good performance of Butler network can be realized.

1. INTRODUCTION

Coupler is an important and fundamental component in microwave circuits and antenna systems [1–15]. Recently, there has been a growing demand for investigating crossover (the special case of coupler) for circuit layout and routing [16–22]. Crossover is used in some systems with special phase requirements, such as Butler beam forming network [23, 24]. The conventional way to meet their phase requirements is employing additional phase shifter, but the phase shifter usually introduces interconnecting mismatch loss and imbalanced amplitude. In this case, a crossover with arbitrary phase delay will make the elimination of the phase shifter possible. It helps to simplify the system structure and improve overall performance.

In this paper, a design procedure for crossover with arbitrary phase delay is provided. It is based on the admittance matrix and described as follows: First, the scattering matrix as well as the admittance matrix

Received 19 July 2013, Accepted 5 November 2013, Scheduled 7 November 2013

* Corresponding author: Ge Tian (tiange.njust@163.com).

is established which are expressed by the characteristic parameters of the crossover. Secondly, the admittance matrix expressed by the crossover physical parameters is deduced. Then, closed-form design formulations are given by letting the two admittance matrices be equal. Finally, a crossover with 45° phase delay is developed as an example. This design method has advantages of simpleness, directness and high efficiency, because the admittance matrix of crossover structure can be established easily due to its definite physical meaning.

2. ADMITTANCE MATRIX APPROACH FOR CROSSOVER DESIGN

Crossover is a special case of couplers, which allows a pair of signals to cross each other while maintaining isolation. It has matching properties at all ports and a given phase delay θ in signal path. Thus the scattering matrix of crossover has the expression as:

$$S = e^{-j\theta} \begin{bmatrix} 0 & 0 & 1 & 0 \\ 0 & 0 & 0 & 1 \\ 1 & 0 & 0 & 0 \\ 0 & 1 & 0 & 0 \end{bmatrix} \quad (1)$$

It is easy to obtain the admittance matrix of the crossover by using S -to- Y matrix transformation with port admittance Y_0 :

$$\begin{aligned} Y &= Y_0 (U - S) (U + S)^{-1} \\ &= jY_0 \begin{bmatrix} -\cot \theta & 0 & \csc \theta & 0 \\ 0 & -\cot \theta & 0 & \csc \theta \\ \csc \theta & 0 & -\cot \theta & 0 \\ 0 & \csc \theta & 0 & -\cot \theta \end{bmatrix} \end{aligned} \quad (2)$$

where U is the unit matrix.

From Equation (2), it is noted that all of the admittance parameters are zero or pure imaginary number, which means the network is lossless. Thus the crossover can be realized using ordinary passive components, such as microstrip lines or lumped components. The admittance matrix is rotational symmetric, which means the crossover structure should be rotational symmetric in the same way.

Following the above guideline, structure in Fig. 1 is chosen to realize the crossover, which is composed of a square ring and inner crossed lines. The corresponding equivalent circuit model is depicted in Fig. 2, in which the characteristic admittance and electric length of the square ring section are Y_a and θ_a . The counterparts of the inner crossed lines are Y_b and θ_b . In order to calculate its admittance matrix,

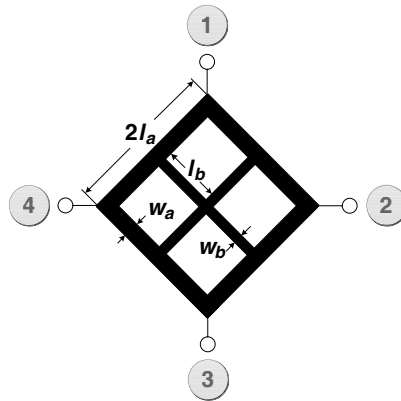


Figure 1. Layout of the crossover.

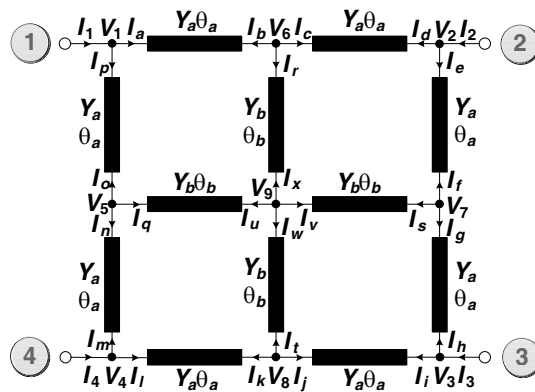


Figure 2. Equivalent circuit model of the crossover.

the relationship between branch currents and node voltages is shown as follows:

$$\begin{cases} I_a = Y_{11}^a V_1 + Y_{12}^a V_6 \\ I_b = Y_{12}^a V_1 + Y_{11}^a V_6 \\ I_c = Y_{11}^a V_6 + Y_{12}^a V_2 \\ I_d = Y_{12}^a V_6 + Y_{11}^a V_2 \\ I_e = Y_{11}^a V_2 + Y_{12}^a V_7 \\ I_f = Y_{12}^a V_2 + Y_{11}^a V_7 \\ I_g = Y_{11}^a V_7 + Y_{12}^a V_3 \\ I_h = Y_{12}^a V_7 + Y_{11}^a V_3 \\ I_i = Y_{11}^a V_3 + Y_{12}^a V_8 \\ I_j = Y_{12}^a V_3 + Y_{11}^a V_8 \\ I_k = Y_{11}^a V_8 + Y_{12}^a V_4 \\ I_l = Y_{12}^a V_8 + Y_{11}^a V_4 \\ I_m = Y_{11}^a V_4 + Y_{12}^a V_5 \\ I_n = Y_{12}^a V_4 + Y_{11}^a V_5 \\ I_o = Y_{11}^a V_5 + Y_{12}^a V_1 \\ I_p = Y_{12}^a V_5 + Y_{11}^a V_1 \end{cases} \quad (3)$$

$$\begin{cases} I_q = Y_{11}^b V_5 + Y_{12}^b V_9 \\ I_u = Y_{12}^b V_5 + Y_{11}^b V_9 \\ I_r = Y_{11}^b V_6 + Y_{12}^b V_9 \\ I_x = Y_{12}^b V_6 + Y_{11}^b V_9 \end{cases} \quad \begin{cases} I_s = Y_{11}^b V_7 + Y_{12}^b V_9 \\ I_v = Y_{12}^b V_7 + Y_{11}^b V_9 \\ I_t = Y_{11}^b V_8 + Y_{12}^b V_9 \\ I_w = Y_{12}^b V_8 + Y_{11}^b V_9 \end{cases}$$

where

$$\begin{cases} Y_{11}^a = -jY_a \cot(\theta_a) \\ Y_{12}^a = jY_a \csc(\theta_a) \\ Y_{11}^b = -jY_b \cot(\theta_b) \\ Y_{12}^b = jY_b \csc(\theta_b) \end{cases}$$

According to Kirchhoff's current law, the following equations can be obtained:

$$\begin{cases} I_b + I_c + I_r = 0 \\ I_f + I_g + I_s = 0 \\ I_k + I_j + I_t = 0 \\ I_o + I_n + I_q = 0 \\ I_x + I_v + I_w + I_u = 0 \\ I_1 = I_a + I_p \\ I_2 = I_d + I_e \\ I_3 = I_i + I_h \\ I_4 = I_l + I_m \end{cases} \quad (4)$$

Based on the definition of admittance matrix, the admittance parameters corresponding to Fig. 2 can be calculated from Equations (3), (4):

$$Y' = \begin{bmatrix} Y_{11} & Y_{12} & Y_{13} & Y_{12} \\ Y_{12} & Y_{11} & Y_{12} & Y_{13} \\ Y_{13} & Y_{12} & Y_{11} & Y_{12} \\ Y_{12} & Y_{13} & Y_{12} & Y_{11} \end{bmatrix} \quad (5)$$

where

$$\begin{aligned} Y_{11} &= 2Y_{11}^a + 2Y_{12} - Y_{13} \\ Y_{12} &= -\frac{(Y_{12}^a)^2 Y_{11}^b}{2Y_{11}^a Y_{11}^b + (Y_{11}^b)^2 - (Y_{12}^b)^2} \\ Y_{13} &= -\frac{(Y_{12}^a)^2 (Y_{12}^b)^2}{(2Y_{11}^a + Y_{11}^b) (2Y_{11}^a Y_{11}^b + (Y_{11}^b)^2 - (Y_{12}^b)^2)} \end{aligned}$$

Letting the admittance matrix (2) be equal to the one in expression (5), three equations with four unknown parameters (Y_a , θ_a , Y_b and θ_b) are obtained. Subsequently, structure parameters can be derived in term of the given phase delay θ :

$$\begin{aligned}\theta_a &= \arctan \sqrt{\frac{3 + \cos \theta}{1 - \cos \theta}} \\ Y_a &= \frac{Y_0}{2} \sqrt{\frac{3 + \cos \theta}{1 + \cos \theta}} \\ \theta_b &= 90^\circ\end{aligned}\quad (6)$$

while Y_b can be arbitrary value.

It can be seen that the crossover structure has some characteristics: the characteristic admittance and electric length of the square ring section are determined by phase delay θ ; the electric length of the inner crossed lines are fixed as 90° ; the characteristic admittance of the inner crossed lines can be arbitrary value, which makes the design more flexible. The relationship between the physical length θ_a of the structure and electric length θ of characteristic is discussed by derivation of Equation (6) as follows:

$$\frac{d\theta_a}{d\theta} = \frac{-\sin \theta}{2\sqrt{(3 + \cos(\theta))(1 - \cos(\theta))}} \quad (7)$$

Thus next conclusions are got:

$$\frac{d\theta_a}{d\theta} < 0 \quad \text{when } \theta \in (0^\circ, 180^\circ) \quad (8)$$

$$\frac{d\theta_a}{d\theta} > 0 \quad \text{when } \theta \in (180^\circ, 360^\circ) \quad (9)$$

The above equations mean that the area of the crossover decreases with increasing θ when $\theta \in (0^\circ, 180^\circ)$, but increases with increasing θ when $\theta \in (180^\circ, 360^\circ)$. The physical length between ports 1 and 3 of the crossover is $2\sqrt{2}\theta_a$ according to Fig. 2, and the electric length of characteristic is θ in Equation (1). In order to make a comparison, variations of $H(\theta) = 2\sqrt{2}\theta_a - \theta$ versus θ is drawn in Fig. 3.

It can be seen that $H(\theta) = 0$ is obtained when $\theta = 137.8^\circ$, which implies that the physical length of the crossover is equal to the electric length of characteristic; the physical length is longer than the electric length when $\theta \in (0^\circ, 137.8^\circ)$; the physical length is shorter than the electric length when $\theta \in (137.8^\circ, 360^\circ)$, which is suitable for compact system.

This section takes a crossover with $\theta = 45^\circ$ phase delay as an example. $Y_b = 0.009S$ is chosen for convenience and the other parameters are calculated as $\theta_a = 74.3^\circ$, $Y_a = 0.015S$ according to formulation (6).

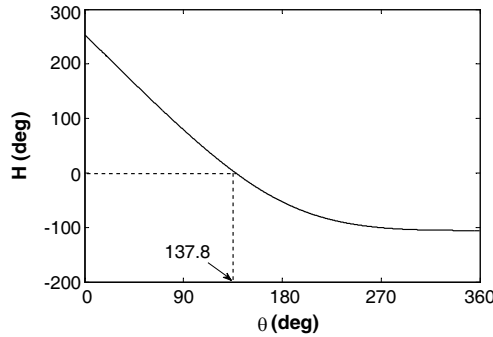


Figure 3. Variations of $H(\theta) = 2\sqrt{2}\theta_a - \theta$ versus θ .

3. RESULTS AND DISCUSSIONS

The crossover is fabricated on Rogers RO4003 substrates with dielectric constant 3.55 and thickness 0.813 mm. Its center frequency is 6 GHz and the geometric parameters are $w_a = 1.1$ mm, $l_a = 7.3$ mm, $w_b = 0.32$ mm, and $l_b = 9.2$ mm.

The frequency responses and phase delay between the diagonal ports (port 1 and 3) are simulated by commercial software CST. The results of simulation and measurement are shown in Fig. 4 and Fig. 5. It can be seen that S_{11} is below -23 dB, while isolation S_{21} is below -25.4 dB at center frequency. The insertion loss of transmission characteristics show $S_{13} = -0.8$ dB and the 15-dB return loss bandwidth is 36%. Measured phase delay between the ports in signal path is 44.2° . Fig. 6 shows the photograph of the fabricated crossover.

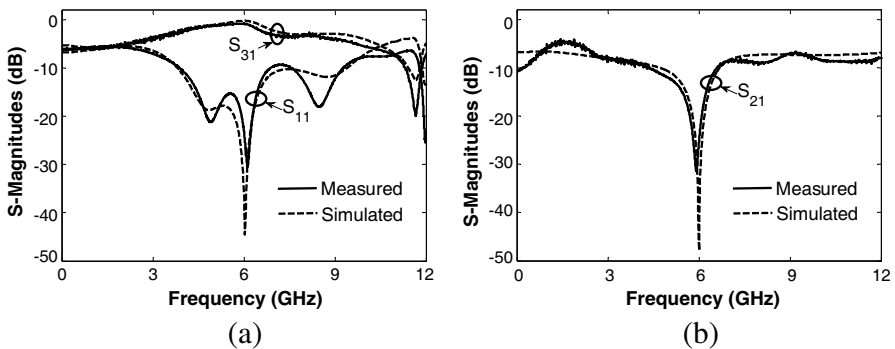


Figure 4. Simulated and measured responses of the crossover.

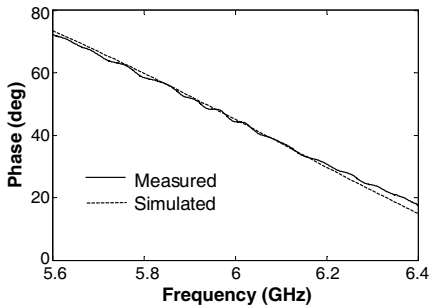


Figure 5. Phase delay between the ports in signal path.

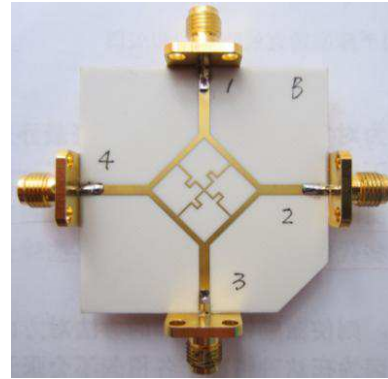


Figure 6. Photograph of the fabricated crossover.

4. CONCLUSION

In this paper, a design method for crossover with arbitrary phase delay is proposed. Based on admittance matrix, closed-form design formulations have been obtained which makes the crossover design very easy. A crossover with 45° phase delay at 6 GHz is designed and fabricated. The measured and simulated results match each other well, and exhibit an accurate phase delay as expected. It should be noted that the proposed admittance matrix approach is suitable not only for the structure in this paper, but also for more other established and new structures.

REFERENCES

1. Zheng, N., L. Zhou, and W.-Y. Yin, "A novel dual-band II-shaped branch-line coupler with stepped-impedance stubs," *Progress In Electromagnetics Research Letters*, Vol. 25, 11–20, 2011.
2. Wong, Y. S., S. Y. Zheng, and W. S. Chan, "Multifolded bandwidth branch line coupler with filtering characteristic using coupled port feeding," *Progress In Electromagnetics Research*, Vol. 118, 17–35, 2011.
3. Han, L., K. Wu, and X.-P. Chen, "Accurate synthesis of four-line interdigitated coupler," *IEEE Trans. on Microw. Theory and Tech.*, Vol. 57, No. 10, 2444–2455, 2009.
4. Xu, H.-X., G.-M. Wang, and J.-G. Liang, "Novel CRLH TL metamaterial and compact microstrip branch-line coupler

- application,” *Progress In Electromagnetics Research C*, Vol. 20, 173–186, 2011.
5. Zhang, J. and X.-W. Sun, “Harmonic suppression of branch-line and rat-race coupler using complementary split ring resonators (CSRR) cell,” *Progress In Electromagnetics Research Letters*, Vol. 2, 73–79, 2008.
 6. Caloz, C., A. Sanada, and T. Itoh, “A novel composite right-/left-handed coupled-line directional coupler with arbitrary coupling level and broad bandwidth,” *IEEE Trans. on Microw. Theory and Tech.*, Vol. 52, No. 3, 980–992, 2004.
 7. Elhiwaris, M. Y. O., S. K. B. A. Rahim, U. A. K. Okonkwo, N. M. Jizat, and M. F. Jamlos, “Miniaturized size branch line coupler using open stubs with high-low impedances,” *Progress In Electromagnetics Research Letters*, Vol. 23, 65–74, 2011.
 8. Zhu, J., Y. Zhou, and J. Liu, “Miniaturization of broadband 3-dB branch-line coupler,” *Progress In Electromagnetics Research Letters*, Vol. 24, 169–176, 2011.
 9. Sun, K.-O., S.-J. Ho, C.-C. Yen, and D. V. D. Weide, “A compact branch-line coupler using discontinuous microstrip lines,” *IEEE Microw. Wirel. Compon. Lett.*, Vol. 15, No. 8, 519–520, 2005.
 10. Liu, G.-Q., L.-S. Wu, and W.-Y. Yin, “A Compact microstrip rat-race coupler with modified lange and T-shaped arms,” *Progress In Electromagnetics Research*, Vol. 115, 509–523, 2011.
 11. Kim, J.-S. and K.-B. Kong, “Compact branch-line coupler for harmonic suppression,” *Progress In Electromagnetics Research C*, Vol. 16, 233–239, 2010.
 12. Kuo, J.-T. and C.-H. Tsai, “Generalized synthesis of rat race ring coupler and its application to circuit miniaturization,” *Progress In Electromagnetics Research*, Vol. 108, 51–64, 2010.
 13. Park, M.-J. and B. Lee, “Design of ring couplers for arbitrary power division with 50Ω lines,” *IEEE Microw. Wirel. Compon. Lett.*, Vol. 21, No. 4, 185–187, 2011.
 14. Hayati, M. and M. Nosrati, “Loaded coupled transmission line approach of left-handed (LH) structures and realization of a highly compact dual-band branch-line coupler,” *Progress In Electromagnetics Research C*, Vol. 10, 75–86, 2009.
 15. Nosrati, M. and B. S. Virdee, “Realization of a compact branch-line coupler using quasi-fractal loaded coupled transmission-lines,” *Progress In Electromagnetics Research C*, Vol. 13, 33–40, 2010.
 16. Yao, J. J., “Nonstandard hybrid and crossover design with branch-line structures,” *IEEE Trans. on Microw. Theory and Tech.*,

- Vol. 58, No. 12, 3801–3808, 2010.
17. Yao, J. J., C. Lee, and S. P. Yeo, “Microstrip branch-line couplers for crossover application,” *IEEE Trans. on Microw. Theory and Tech.*, Vol. 59, No. 1, 87–92, 2011.
 18. Shao, J., H. Ren, B. Arigong, C. Z. Li, and H. L. Zhang, “A fully symmetrical crossover and its dual-frequency application,” *IEEE Trans. on Microw. Theory and Tech.*, Vol. 60, No. 8, 2410–2416, 2012.
 19. Wong, F. L. and K. K. M. Cheng, “A novel, planar, and compact crossover design for dual-band applications,” *IEEE Trans. on Microw. Theory and Tech.*, Vol. 59, No. 3, 568–573, 2011.
 20. Chiou, Y. C., J. T. Kuo, and H. R. Lee, “Design of compact symmetric four-port crossover junction,” *IEEE Microw. Wirel. Compon. Lett.*, Vol. 19, No. 9, 545–547, 2009.
 21. Chen, Y. and S.-P. Yeo, “A symmetrical four-port microstrip coupler for crossover application,” *IEEE Trans. on Microw. Theory and Tech.*, Vol. 55, No. 11, 2434–2438, 2007.
 22. Lee, Z.-W. and Y.-H. Pang, “Compact planar dual-band crossover using two-section branch-line coupler,” *Electron. Lett.*, Vol. 48, No. 21, 1348–1349, 2012.
 23. Chen, W.-L., G.-M. Wang, and C.-X. Zhang, “Fractal-shaped switched-beam antenna with reduced size and broadside beam,” *Electron. Lett.*, Vol. 44, No. 19, 1110–1111, 2008.
 24. He, J., B.-Z. Wang, Q.-Q. He, Y.-X. Xing, and Z.-L. Yin, “Wideband X-band microstrip butler matrix,” *Progress In Electromagnetics Research*, Vol. 74, 131–140, 2007.